

Solid state synthesis and catalytic performance of pyrochlore

 $\text{Er}_2\text{Ti}_2\text{O}_7$ in epoxidation of cyclooctene

Maryam Hasanzadeh Esfahani, Mahdi Behzad*

Faculty of chemistry, Semnan University, Semnan, Iran

Article history:

Received: 27/Jan/2020

Received in revised form: 18/Feb/2020

Accepted: 23/Feb/2020

Abstract

$\text{Er}_2\text{Ti}_2\text{O}_7$ pyrochlore structure was successfully prepared by solid-state method. The prepared microstructure mixed-metal oxide was characterized by XRD, SEM, EDX, FT-IR and BET. X-ray powder diffraction revealed a Cubic crystal system with $Fd3m$ space group for $\text{Er}_2\text{Ti}_2\text{O}_7$. The morphology and mean particle size of the sample was characterized by the scanning electron microscope. The elemental analysis or chemical characterization of the sample was determined by Energy Dispersive X-ray microanalysis. The absorption bands between the A and B sites in the pyrochlore structure were confirmed by Fourier transmission infrared spectra in (400–4000 cm^{-1}) range. The specific surface area and the pore size distributions of the sample were calculated using Brunauer–Emmett–Teller (BET) method and Barrett–Joyner–Halenda (BJH) method respectively. The complex has been used as a catalyst for epoxidation of cyclooctene with TBHP (tert-butyl hydroperoxide). Various parameters including catalyst amount, solvent type and amount, oxidant/substrate ratio and time have been optimized and almost. Considerable catalytic activity and high epoxide selectivity has been found.

Keywords: pyrochlore; solid state; X-ray diffraction; catalyst; Epoxidation.

1. Introduction

$\text{RE}_2\text{Ti}_2\text{O}_7$ titanates (RE stands for rare earth) belong to the family of pyrochlore mixed-metal oxides with general formula $\text{A}_2\text{B}_2\text{O}_7$ in which, the crystal structure could be considered as the superstructure of defect fluorite lattice [1-4]. Among various applications of $\text{RE}_2\text{Ti}_2\text{O}_7$ mixed-metal oxides are their applications as electrolytes for solid oxide fuel cells [5,6], catalysis [7-9], Photocatalytic activity, photoluminescence, and several other potential applications have also been investigated which has made them as suitable candidates for industrial applications [10-15].

Different synthetic approaches have been used for the synthesis of $\text{Ln}_2\text{Ti}_2\text{O}_7$ oxides. Solid state reaction at elevated temperatures is the most widely studied route

[16-18]. Other methods including sol-gel [19-23], polymerized complex method [24,25], high energy ball milling [26,27] and pulsed laser deposition [28,29] have also been well explored, however, the formation of undesirable side products and the left-over starting materials, as well as the requirement of complicated equipment and long reaction times caused by multiple steps are the drawback of such methods. Epoxidation of alkenes, on the other hands, is a very important industrial reaction which has received great attention [30-35]. Various catalyst have been explored for such reactions including metal oxides [36], supported metal oxides [37], transition metal complexes [38-40] and immobilized transition metal complexes [41-43], etc. TiO_2 is one of the metal oxides which is extensively

*.Corresponding author: Associate Professor of Inorganic Chemistry, Faculty of Chemistry, Semnan University, Semnan, Iran
mbehzad@semnan.ac.ir

used both as unsupported and supported catalyst for epoxidation of alkenes and cycloalkenes. On the other hand, our literature survey did not show the use Er_2O_3 as alkene epoxidation catalyst. Besides, to the best of our knowledge, mixed metal oxides-catalyzed epoxidation of cyclooctene is also very scarcely or not explored in literature. Hence, in this work we report the solid state synthesis of $\text{Er}_2\text{Ti}_2\text{O}_7$ micro-structured material. $\text{Er}_2\text{Ti}_2\text{O}_7$ was characterized by PXRD, SEM, EDX and FTIR. The synthesized material was used as potential catalyst for the epoxidation of cyclooctene. Several reaction conditions were optimized by a one-at-a-time approach. Considerable catalytic activity was achieved at the optimized conditions. Besides high epoxide selectivity was also obtained.

2. Experimental

2.1. Catalyst preparation

Powders Erbium oxide Er_2O_3 (99.99% purity), titanium oxide TiO_2 (99.99% purity) were pre-annealed at various temperatures to remove hydroxides before mixing. Then 3.7 mmol (1.41g) of Er_2O_3 and 7.5 mmol (0.59g) of TiO_2 were mixed, ground into a uniform powder using a mortar and pestle, and made into rods using cylindrical balloons. A vacuum pump was used to remove any air inside the balloon, and the rods were pressed in a hydrostatic press at 60 MPa for 10 minutes, and sintered with O_2 Pressure at temperatures 1350 °C for 48 hours. 1.95g (98.00%) of the pink colored target material was collected.

2.2. Spectroscopic Characterization

Powder diffraction data was taken in a PANalytical X'Pert system, which uses copper K-alpha radiation with wavelength 1.5406 Å. The morphology of the sample was characterized by the scanning electron microscope (SEM) on a TESCAN Vega LSU microscope equipped with an Oxford X-Max detector. Energy Dispersive X-ray microanalysis (EDX) was taken by the Oxford detector. Fourier transmission infrared spectra (400–4000 cm^{-1}) of KBr powder pressed pellet was obtained on a Shimadzu 8400S FT-IR instrument. The Brunauer–Emmett–Teller (BET) surface area (S_{BET}) was obtained by nitrogen

adsorption–desorption test of the sample at 77 K on a BELSORP MINI II system.

2.3. General oxidation reaction

$\text{Er}_2\text{Ti}_2\text{O}_7$ has been used as a catalyst in different reaction condition for oxidation of cyclooctene by tert-butyl hydroperoxide (TBHP) as oxidant. In the absence of the complex, a little oxidation product has been observed. The retention times for the starting materials and the products have been obtained by pure and Merck samples. The progress of the reaction has been monitored by GC (Gas chromatography). The conversion percentages (%) and Selectivity have been calculated according to the following equations, that C_{initial} is initial concentration and C_{final} is final concentration of cyclooctene (substrate). In a typical experiment, 10 μmol of pyrochlore catalyst was dissolved in 5 mL of freshly distilled methanol and then 10 mmol of cyclooctene and 20 mmol of TBHP were added. The reaction mixtures were refluxed while being stirred and the reaction progress was monitored at 60 min intervals.

$$\text{Conv.(\%)} = \frac{C_{\text{init}}(\text{alkene}) - C_{\text{final}}(\text{alkene})}{C_{\text{init}}(\text{alkene})} \times 100$$

$$\text{Sel.(\%)} = \frac{C_{\text{final}}(\text{epoxide})}{C_{\text{init}}(\text{alkene}) - C_{\text{final}}(\text{alkene})} \times 100$$

3. Results and discussion

3.1. XRD analysis

The crystalline phase structure between 10 to 90° with step size and step time 0.017, 120 s respectively was determined by powder X-ray diffraction technique. All the reflections in the diffractogram of the sample are recorded to the cubic phase of space group $Fd\bar{3}m$ without any impurity phase (JCPDS: 73-1647). The result of the Qualitative phase analysis obtained from the X'Pert High Score program has been shown in Table 1. Powder XRD data Structural analysis has been done by the Rietveld refinement method using MAUD software [44]. Factor R was obtained after a few cycles of refinement of zero-point correction, scale factors, background polynomial coefficients, peak width, and the pseudo-Voigt profile parameters.

The output of the refinement of the $\text{Er}_2\text{Ti}_2\text{O}_7$ oxide has been shown in Table 2. The black circles for the experimental peaks and the red lines for the calculated peaks and the blue lines represent the difference between the experimental peaks and the calculated ones. Perpendicular black lines correspond to Bragg reflections in Fig 1. The mean crystallite size of the sample was calculated from the XRD (2 2 2) peak with Scherrer equation [45-48]. $D = 0.89\lambda/\beta \cos \Theta$, where D is the average crystallite size in nm, λ is the Cu $K\alpha$ wavelength, β is Full width at half maximum of the peak in rad and Θ is the corresponding diffraction angle.

3.2. Scanning electronic microscopy

The mean particle sizes of $\text{Er}_2\text{Ti}_2\text{O}_7$ powder obtained by a scanning electron microscope (SEM) is estimated to be about 1.5 μm by Digimizer program. SEM micrograph and Histogram diagram have been shown in Fig 2. The Sample consists basically of micron size agglomerates of irregular shape. EDX micrograph of $\text{Er}_2\text{Ti}_2\text{O}_7$ sample has been shown in Fig 3. Energy Dispersive X-ray microanalysis is an analytical technique used for the elemental analysis or chemical characterization of a sample. Chemical composition from EDX analyses confirms Er/Ti molar ratio close to 1. Table 3 shows Weight percent and atomic percent of elements.

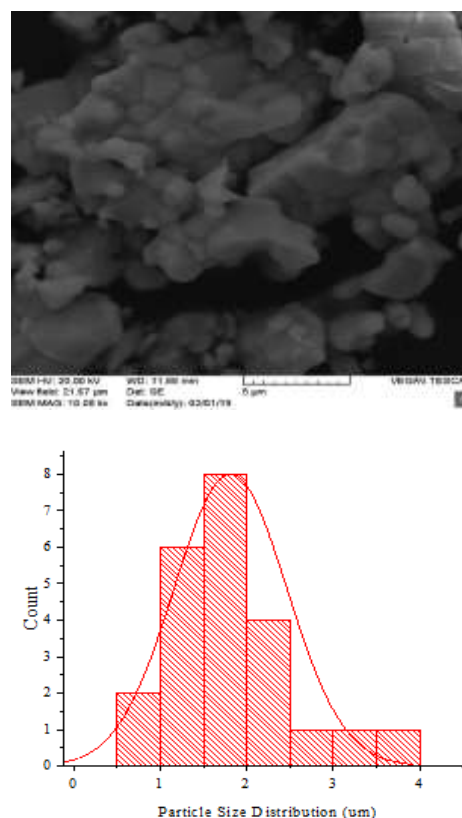


Fig 2. Scanning electron micrographs and Histogram diagram of the $\text{Er}_2\text{Ti}_2\text{O}_7$ powder.

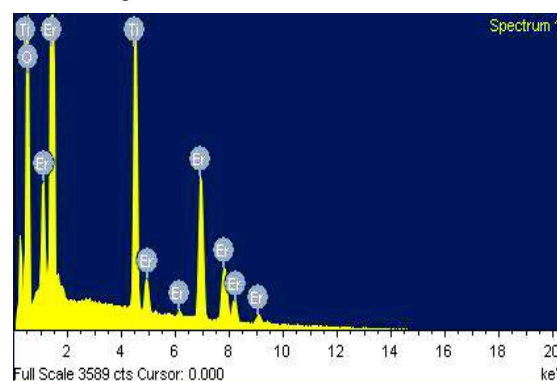


Fig 3. EDX analysis of the $\text{Er}_2\text{Ti}_2\text{O}_7$ sample.

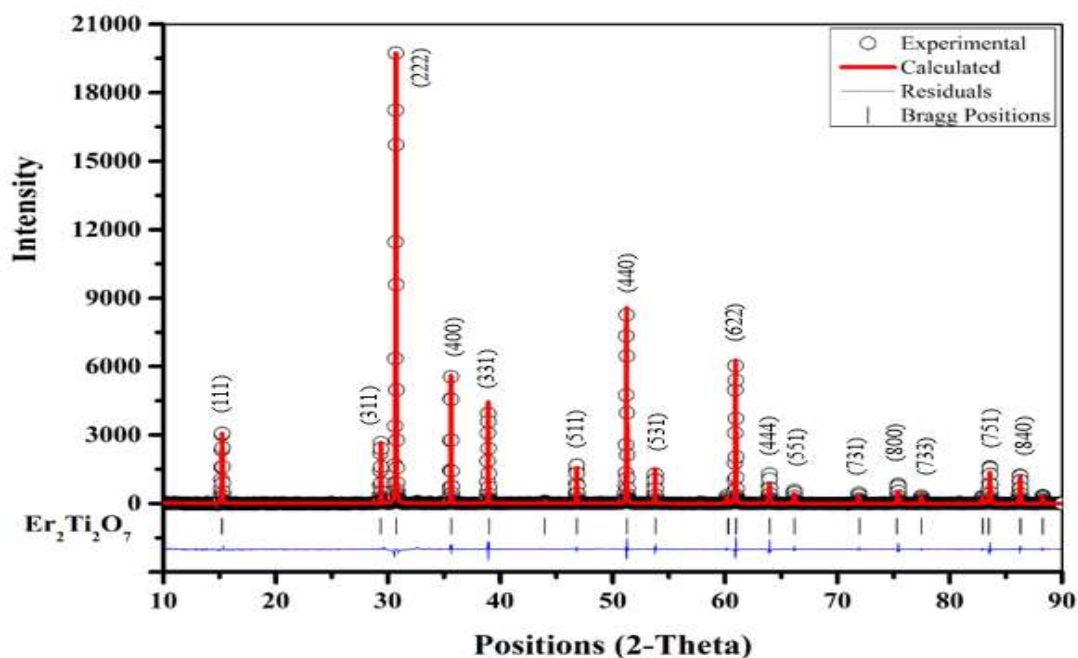


Fig 1. X-ray powder diffraction pattern of the prepared pyrochlore at 1350°C

Table 1. Results of Qualitative phase analysis obtained from X'Pert High Score program.

Formula	JCPDS Code	Cell Parameters	Space Group	Crystal Structure
$\text{Er}_2\text{Ti}_2\text{O}_7$	01-73-1647	$a = 10.0762\text{\AA}$	$Fd\bar{3}m$	Cubic

Table 2. Results of Rietveld Quantitative phase analysis obtained from MAUD.

Phase	Cell Parameters	Crystallite size	R _{wp}	R _{exp}	GOF	R _{Bragg}
$\text{Er}_2\text{Ti}_2\text{O}_7$	$a = 10.0776\text{\AA}$	116 nm	7.4	5.6	1.32	4.68

3.3. Infrared spectral studies

FT-IR spectroscopy has been used for studying the nature of metal-oxygen bonds in the pyrochlore oxides. There are usually seven IR-active optic modes in the pyrochlore compounds in the range of 100–1000 cm^{-1} . The band (ν_1) at about 100 cm^{-1} is related to the O'-A-O' bending vibration. The band (ν_2) at about 150 cm^{-1} is related to the O-A-O bending vibration. The band (ν_3) at about 200 cm^{-1} is related to the A-BO₆ stretching vibration. The band (ν_4) at about 300 cm^{-1} is related to the O-B-O bending vibration, the band (ν_5) at about 400 cm^{-1} is related to the A-O stretching vibration in the AO₆O'₂ polyhedron of A₂B₂O₇. The band (ν_6) at about 500 cm^{-1} is related to the A-O' stretching vibration. The band (ν_7) at about 600 cm^{-1} is related to the B-O stretching vibration in the BO₆ octahedron [49-52]. Peak position and types of the corresponding vibrational modes in erbium titanate pyrochlore in the

400–4000 cm^{-1} range has been shown in Fig 4 and Table 4.

Table 3. Results of the Weight percent and atomic percent of elements of the $\text{Er}_2\text{Ti}_2\text{O}_7$ sample.

Atoms	Weight%			Atomic%		
	O	Ti	Er	O	Ti	Er
$\text{Er}_2\text{Ti}_2\text{O}_7$	35.93	14.91	49.15	78.77	10.92	10.31

Table 4. Peak position and types of the corresponding vibrational modes (cm^{-1}).

Chemical Formula	ν (Re-O')	ν (Ti-O)
$\text{Er}_2\text{Ti}_2\text{O}_7$	473	576

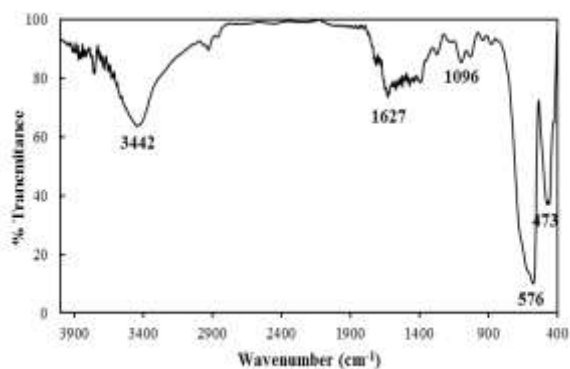


Fig 4. IR spectra of the synthesized sample at 1350°C.

3.4. BET surface area

The specific BET surface area of the $\text{Er}_2\text{Ti}_2\text{O}_7$ sample obtained from N_2 adsorption-desorption test at 77 K is $0.841 \text{ m}^2\text{g}^{-1}$. The small surface area was consequences of used specific method during the synthesis of pyrochlore. Surface area, Total pore volume and Mean pore diameter from BET method and radius pore, volume pore and area pore from BJH method have been shown in Tables 5 and 6. Nitrogen adsorption-desorption isotherm plot has been shown in Fig 5.

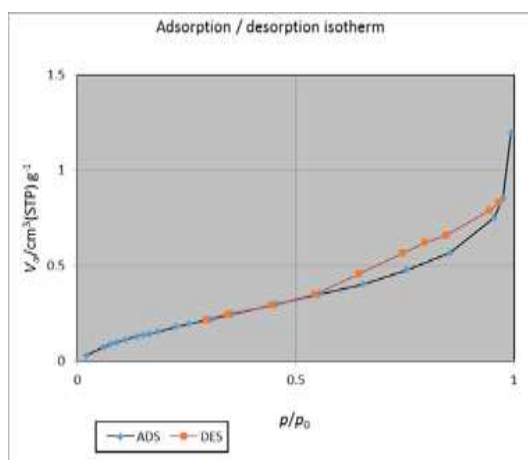


Fig 5. N_2 adsorption-desorption isotherm plot

Table 6. The BJH analysis results of $\text{Er}_2\text{Ti}_2\text{O}_7$ sample

Volume pore	Radius pore	Area pore
$0.0018 \text{ (cm}^3\text{g}^{-1})$	1.22 (nm)	$0.947 \text{ (m}^2\text{g}^{-1})$

Table 5. The BET analysis results of $\text{Er}_2\text{Ti}_2\text{O}_7$ sample

Surface area (a_s)	Total pore volume ($p/p_0=0.99$)	Mean pore diameter
$0.841 \text{ (m}^2\text{g}^{-1})$	$0.0017 \text{ (cm}^3\text{g}^{-1})$	8.310 (nm)

3.5. Catalytic activity

Various reaction conditions including amount of catalyst, solvent type, solvent amount, reaction time, and oxidant to substrate ratio were optimized. In a typical experiment, $10 \mu\text{mol}$ of the complex was dissolved in 5 mL of freshly distilled methanol and then 10 mmol of cyclooctene and 20 mmol of TBHP were added. The reaction mixture was refluxed while being stirred and the reaction progress was monitored at 60 minute intervals by GC up to 30 h. The optimized reaction time was found to be 24 hours. Then, the amount of the catalyst was optimized and the optimized amount was found to be $15 \mu\text{mol}$. The catalytic reaction was also performed in different solvents such as ethanol, methanol, acetonitrile and chloroform. Methanol was found as the best solvent. Then, the amount of solvent was optimized and Solvent-free had the best result. The oxidant to substrate ratio was then optimized and 2:1 oxidant: substrate ratio was found as the optimized ratio. The results of the optimization of parameters such as catalyst amount, the solvent type, solvent amount and the oxidant to substrate ratio have been shown in Fig 6. And the result of epoxidation selectivity has been shown in Table 7.

Table 7. The result of the epoxidation selectivity of sample

Pyrochlore	Conversion percent	Selectivity	
		Epoxide	Other products
$\text{Er}_2\text{Ti}_2\text{O}_7$	77	84.4	15.6

Conditions: $15 \mu\text{mol}$ of catalyst, 10 mmol cyclooctene, 20 mmol TBHP, reflux 24h without solvent.

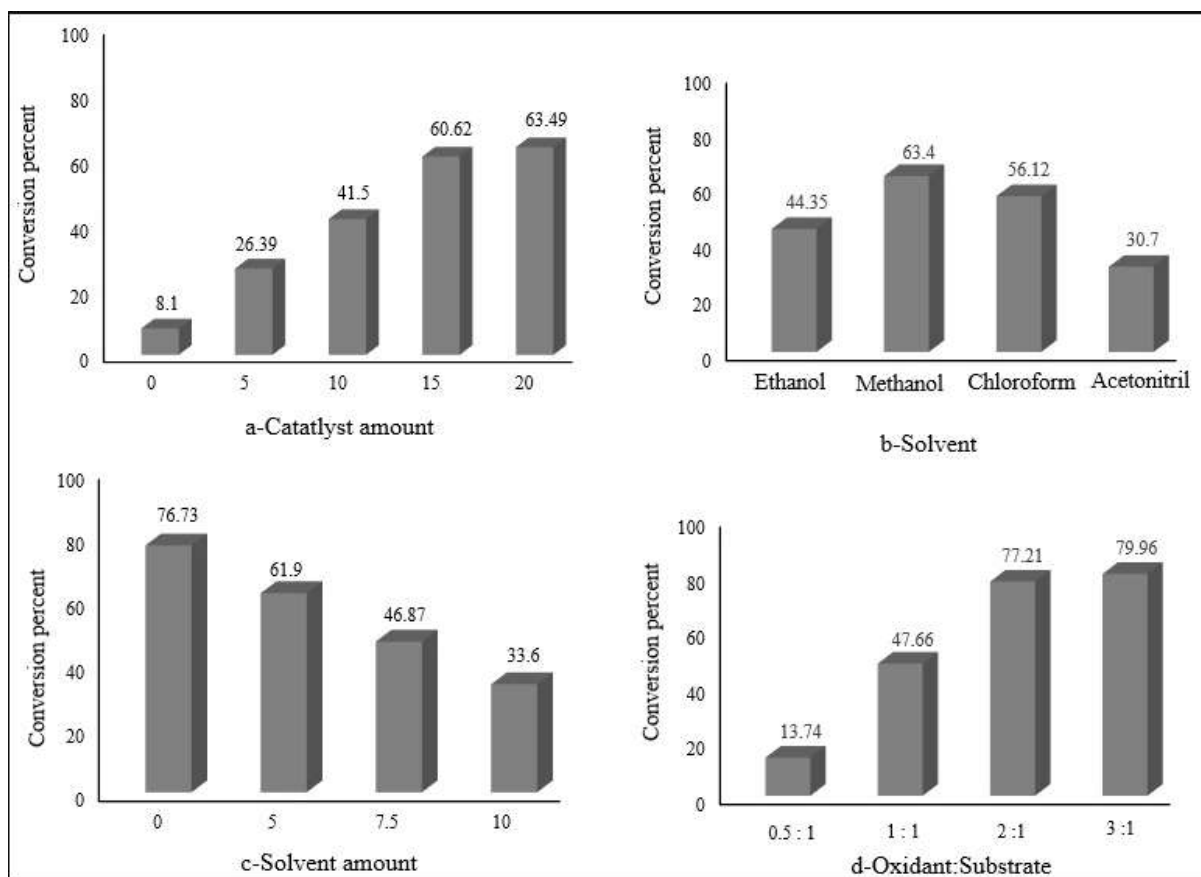


Fig 6. The results of the optimization: (a) Catalyst amount (b) Solvent type (c) Solvent amount (d) Oxidant: Substrate

To show the merit of the work, a comparison is made with some previously reported metal oxide catalysts and the results are collected in table 8. As could be seen, the studied catalyst has shown almost better catalytic performance both in terms of conversion percent and epoxide selectivity.

4. Conclusions

$\text{Er}_2\text{Ti}_2\text{O}_7$ pyrochlore was successfully synthesized by solid state method without any impurity with cubic system and $Fd\bar{3}m$ space group in region 10 to 90 with low step size and high step time. The existence of (331) and (511) peaks confirm pyrochlore structure [55]. The analysis results show that the sample had similar

microparticle sizes, small specific surface area, and porous structure. $\text{Er}_2\text{Ti}_2\text{O}_7$ shows the high catalytic activity for epoxidation of cyclooctene. The activity of epoxidation of $\text{Er}_2\text{Ti}_2\text{O}_7$ seems to be due to Er and Ti elements on the surface of pyrochlore. Observed catalytic activities for $\text{Er}_2\text{Ti}_2\text{O}_7$ could be related to crystal structure, high crystallinity and Er 4f shell.

Acknowledgement

The research leading to these results has received funding from the Iran National Science Foundation (INSF) under the grant agreement no 94802577.

Table 8. Comparison of the epoxidation performance of the studied catalyst with some literature data.

Catalyst	Substrate	Oxidant	Solvent	Approximate conversion%	Epoxide selectivity%	Reference
Mesoporous synthetic TiO ₂	Cyclohexene	H ₂ O ₂	<i>tert</i> -Butanol	39	58	53
Commercial Ishihara ST-01 TiO ₂	Cyclohexene	H ₂ O ₂	<i>tert</i> -Butanol	17	30	53
Commercial Degussa ST-01 TiO ₂	Cyclohexene	H ₂ O ₂	<i>tert</i> -Butanol	24	35	53
RuO ₂ /TiO ₂	Cyclohexene	H ₂ O ₂	<i>tert</i> -Butanol	34	78	53
Anatase TiO ₂	Cyclooctene	H ₂ O ₂ / UV light	CH ₃ CN	35	97	54
Er ₂ Ti ₂ O ₇	Cyclooctene	TBHP	-	77	84.4	This work

References

- [1] V. S. Maryasin. M. E. Zhitomirsky. *Phys. Rev. B.* **90** (2014) 094412.
- [2] V. V. Popov. A. P. Menushenkov. B. R. Gaynanov. A. A. Ivanov. F. dAcapito. A. Puri. I. V. Shchetinin. M. V. Zheleznyi. M. M. Berdnikova. A. A. Pisarev. A. A. Yastrebsev. N. A. Tsarenko. L. A. Arzhatkina. O. D. Horozova. I. G. Rachenok. K. V. Ponkratov. *J. Alloys. Compd.* **746** (2018) 377.
- [3] R. C. Ewing. W. J. Weber. J. Lian. *J. Appl. Phys.* **95** (2004) 5949.
- [4] V. V. Popov. A. P. Menushenkov. A. A. Ivanov. B. R. Gaynanov. A. A. Yastrebsev. F. dAcapito. A. Puri. G. R. Castro. I. V. Shchetinin. M. V. Zheleznyi. Ya. V. Zubavichus. K. V. Ponkratov. *J. Phys. Chem. Solids.* **130** (2019) 144.
- [5] M. Mori. G. M. Tompsett. N. M. Sammes. E. Suda. Y. Takeda. *Solid. State. Ion.* **158** (2003) 79.
- [6] M. Kumar. I. A. Raj. R. Pattabiraman. *Mater. Chem. Phys.* **108** (2008) 102.
- [7] S. H. Oh. R. Black. E. Pomerantseva. J. H. Lee. L. F. Nazar. *Nat. Chem.* **4** (2012) 1004.
- [8] J. Tian. H. Peng. X. Xu. W. Liu. Y. Ma. X. Wang. X. Yang. *Catal. Sci. Technol.* **5** (2015) 2270.
- [9] K. Fujii. Y. Sato. S. Takase. Y. Shimizu. *J. Electrochem. Soc.* **162** (2015) F129.
- [10] W. Ragsdale. S. Gupta. K. Conard. S. Delacruz. V. R. Subramanian. *Appl. Catal. B Environ.* **180** (2016) 442.
- [11] Q. Wang. X. Cheng. J. Li. H. Jin. *J. Photochem. Photobiol. A. Chem.* **321** (2016) 48.
- [12] M. Bencina. M. Valant. *J. Am. Ceram. Soc.* **101** (2018) 82.
- [13] Z. Shao. S. Saitzek. J.-F. Blach. A. Sayede. P. Roussel. R. Desfeux. *Eur. J. Inorg. Chem.* **2011** (2011) 3569.
- [14] S. K. Mahesh. P. P. Rao. M. Thomas. T. L. Francis. P. Koshy. *Inorg. Chem.* **52** (2013) 13304.
- [15] A. Garbout. T. Turki. M. Ferid. *J. Lumin.* **196** (2018) 326.
- [16] O. A. S. Ahmed. A. Tairi. A. Chagraoui. S. Khairoun. J. C. Champarnaud-Mesjard. B. Frit. *Ann. Chim. Sci. Mater.* **25** (2000) 201.

- [17] M. K. Ehlert. J. E. Greedan. M. Subramanian. *J. Solid. State. Chem.* **75** (1988) 188.
- [18] B. J. Ismunandar. B. A. Kennedy. J. Hunter. *J. Solid. State. Chem.* **130** (1997) 81.
- [19] A. Kahoul. P. Nkeng. A. Hammouche. F. Naamoune. G. Poillerat. *J. Solid. State. Chem.* **161** (2001) 379.
- [20] Z. S. Chen. W. P. Gong. T. F. Chen. S. L. Li. *Bull. Mater. Sci.* **34** (2011) 429.
- [21] Sh. Wang. W. Li. S. Wang. Z. Chen. *J. Eur. Ceram. Soc.* **35** (2015) 105.
- [22] J. K. Joseph. K. R. Dayas. S. Damodar. B. Krishnan. K. Krishnankutty. V. P. N. Nampoori. *Spectrochim. Acta. A.* **71** (2008) 1281.
- [23] Z.M. Shao. S. Saitzek. P. Roussel. O. Mentre. F. P. Gheorghiu. L. Mitoseriu. R. Desfeux. *J. Solid. State. Chem.* **183** (2010) 1652.
- [24] W. M. Hou. Y. Ku. *J. Alloys. Compd.* **509** (2011) 5913.
- [25] Z. H. Li. H. Xue. X. X. Wang. X. Z. Fu. *J. Mol. Catal.* **206** (2006) 56.
- [26] A. F. Fuentes. Kh. Boulahya. M. Maczka. J. Hanuza. U. Amador. *Solid. State. Sci.* **7** (2005) 343.
- [27] E. Rodriguez-Reyna. A. F. Fuentes. M. Maczka. J. Hanuza. K. Boulahya. U. Amador. *J. Solid. State. Chem.* **179** (2006) 522.
- [28] A. Bayart. S. Saitzek. A. Ferri. R. Pouhet. M. H. Chambrier. P. Roussel. R. Desfeux. *Thin. Solid. Films.* **553** (2014) 71.
- [29] S. Havelia. S. Wang. K. R. Balasubramaniam. P. A. Salvador. *J. Solid. State. Chem.* **182** (2009) 1603.
- [30] K. Jin, J.H. Maalouf, N. Lazouski, N. Corbin, D. Yang, K. Manthiram, *J. Am. Chem. Soc.* **141** (2019) 6413.
- [31] M. Herbert, A. Galindo, F. Montilla, *Catal. Commun.* **8** (2007) 987.
- [32] G. Grigoropoulou, J.H. Clark, J.A. Elings, *Green. Chem.* **5** (2003) 1.
- [33] M. Sankaralingam, M. Balamurugan, M. Palaniandavar, *Coord. Chem. Rev.* **403** (2020) 213085.
- [34] W. Yan, G. Zhang, H. Yan, Y. Liu, X. Chen, X. Feng, X. Jin, C. Yang, *ACS Sustain. Chem. Eng.* **6** (2018) 4423.
- [35] J.M. Asensio, D. Bouzouita, P.W.N.M. van Leeuwen, B. Chaudret, *Chem. Rev.* **120** (2020) 1042.
- [36] A. Blanckenberg, R. Malgas-Enus, *Catal. Rev.* **61** (2019) 27.
- [37] S. Thongboon, P. Rittiron, D. Kiatsaengthong, T. Chukeaw, A. Seubsai, *J. Nanosci. Nanotech.* **20** (2020) 3466.
- [38] S. Shaw, J.D. White, *Chem. Rev.* **119** (2019) 9381.
- [39] Z. Abbasi, M. Behzad, A. Ghaffari, H.A. Rudbari, G. Bruno, *Inorg. Chim. Acta*, **414** (2014) 78.
- [40] W. Al Zoubi, Y.G. Ko, *J. Organomet. Chem.* **822** (2016) 173.
- [41] A. Bezaatpour, M. Behzad, V. Jahed, M. Amiri, Y. Mansoori, Z. Rajabalizadeh, S. Sarvi, *React. Kinet. Mech. Catal.* **107** (2012) 367.
- [42] E. Ahadi, H. Hosseini-Monfared, C. Schlüsener, C. Janiak, A. Farokhi, *Catal. Lett.* **150** (2020) 861.
- [43] S. Tangestaninejad, M. Moghadam, V. Mirkhani, I. Mohammadpoor-Baltork, K. Ghani, *Inorg. Chem. Commun.* **11** (2008) 270.

- [44] L. Lutterotti, S. Matthies, H.R. Wenk, "MAUD: a friendly Java program for material analysis using diffraction," *IUCr Newsl. CPD*. **21** (1999).
- [45] Y. Tao. G. W. Zhao. W. P. Zhang. S. D. Xia. *Mater. Res. Bull.* **32** (1997) 501.
- [46] K. K. Rao. T. Banu. T. Banu. M. Vithal. G. Y. S. K. Swamy. K. R. Kurnar. *Mater. Lett.* **54** (2002) 205.
- [47] S. Brunauer. P.H. Emmett. E. Teller. *J. Am. Chem. Soc.* **60** (1938) 309.
- [48] P. Zhang. *J. Phys. Chem.* **112** (2008) 932.
- [49] M. A. Subramanian. G. Aravamudan. G. V. S. Rao. *Prog. Solid. State. Chem.* **15** (1983) 55.
- [50] H. Du. X. Yao. *J. Electroceram.* **9** (2002) 117.
- [51] H. Du. X. Yao. L. Zhang. *Ceram. Int.* **28** (2002) 231.
- [52] M. Chen. D.B. Tanner. J.C. Nino. *Phys. Rev. B.* **72** (2005) 054303 DOI: 10.1103/PhysRevB.72.054303.
- [53] T. Sreethawong, Y. Yamada, T. Kobayashi, S. Yoshikawa, *J. Mol. Catal. A Chem.* **241** (2005) 23.
- [54] C. Yang, X. Lang, W. Ma, C. Chen, H. Ji, J. Zhao, *Chem. Eur.* **20** (2014) 6277.
- [55] Y. Tong. J. Zhu. L. Lu. X. Wang. X. Yang. *J. Alloys. Compd.* **465** (2008) 280.

